

Hasan Kırmızıbekmez<sup>1</sup>İhsan Çalış<sup>1</sup>Remo Perozzo<sup>2</sup>Reto Brun<sup>3</sup>Ali A. Dönmez<sup>4</sup>Anthony Linden<sup>5</sup>Peter Rüedi<sup>5</sup>Deniz Tasdemir<sup>5</sup>

# Inhibiting Activities of the Secondary Metabolites of *Phlomis brunneogaleata* against Parasitic Protozoa and Plasmodial Enoyl-ACP Reductase, a Crucial Enzyme in Fatty Acid Biosynthesis

## Abstract

Anti-plasmodial activity-guided fractionation of *Phlomis brunneogaleata* (Lamiaceae) led to the isolation of two new metabolites, the iridoid glycoside, brunneogaleatoside and a new pyrrolidinium derivative (2*S*,4*R*)-2-carboxy-4-(*E*)-*p*-coumaroyloxy-1,1-dimethylpyrrolidinium inner salt [(2*S*,4*R*)-1,1-dimethyl-4-(*E*)-*p*-coumaroyloxypyrrolidine inner salt]. Moreover, a known iridoid glycoside, ipolamiide, six known phenylethanoid glycosides, verbascoside, isoverbascoside, forsythoside B, echinacoside, glucopyranosyl-(1→*G*<sub>1</sub>-6)-martynoside and integrifolioside B, two flavone glycosides, luteolin 7-*O*-β-*D*-glucopyranoside (**10**) and chrysoeriol 7-*O*-β-*D*-glucopyranoside (**11**), a lignan glycoside liriodendrin, an acetophenone glycoside 4-hydroxyacetophenone 4-*O*-(6'-*O*-β-*D*-apiofuranosyl)-β-*D*-glucopyranoside and three caffeic acid esters, chlorogenic acid, 3-*O*-caffeoylquinic acid methyl ester and 5-*O*-caffeoylshikimic acid were isolated. The structures of the pure compounds were elucidated by means of spectroscopic methods (UV, IR, MS, 1D and 2D NMR, [ $\alpha$ ]<sub>D</sub>) and X-ray crystallography. Compounds **10** and **11** were determined to be the major anti-malarial principles of the crude extract (IC<sub>50</sub> values of 2.4 and 5.9 μg/mL, respectively). They also exhibited

significant leishmanicidal activity (IC<sub>50</sub> = 1.1 and 4.1 μg/mL, respectively). The inhibitory potential of the pure metabolites against plasmodial enoyl-ACP reductase (FabI), which is the key regulator of type II fatty acid synthases (FAS-II) in *P. falciparum*, was also assessed. Compound **10** showed promising FabI inhibiting effect (IC<sub>50</sub> = 10 μg/mL) and appears to be the first anti-malarial natural product targeting FabI of *P. falciparum*.

## Key words

*Phlomis brunneogaleata* · Lamiaceae · iridoid · pyrrolidinium derivative · betonicine · luteolin 7-*O*-β-*D*-glucopyranoside · *Plasmodium falciparum* enoyl-acyl carrier protein reductase (FabI) · type II fatty acid synthase (FAS-II)

## Abbreviations

ACP: Acyl Carrier Protein  
CC: Column Chromatography  
FabI: Enoyl-Acyl Carrier Protein Reductase  
FAS-I: Type I Fatty Acid Synthase System  
FAS-II: Type II Fatty Acid Synthase System  
MPLC: Medium Pressure Liquid Chromatography

## Affiliation

<sup>1</sup> Department of Pharmacognosy, Faculty of Pharmacy, Hacettepe University, Ankara, Turkey

<sup>2</sup> Department of Chemistry and Applied Biosciences, ETH Zurich, Zürich, Switzerland

<sup>3</sup> Department of Medical Parasitology and Infection Biology, Swiss Tropical Institute, Basel, Switzerland

<sup>4</sup> Department of Biology, Faculty of Science, Hacettepe University, Ankara, Turkey

<sup>5</sup> Institute of Organic Chemistry, University of Zurich, Zürich, Switzerland

## Correspondence

Dr. Deniz Tasdemir · Institute of Organic Chemistry · University of Zurich · Winterthurerstrasse 190 · 8057 Zurich · Switzerland · Phone: +41-1-635-4213 · Fax: +41-1-635-6812 · E-mail: deniz@oci.unizh.ch

Received December 29, 2003 · Accepted April 12, 2004

## Bibliography

Planta Med 2004; 70: 711–717 · © Georg Thieme Verlag KG Stuttgart · New York  
DOI 10.1055/s-2004-827200  
ISSN 0032-0943

## Introduction

Malaria is a major infectious disease causing more than 1 million deaths and 300 to 500 million clinical infections annually. Parasite resistance is developing rapidly and has resulted in a resurgence of malaria. Therefore, new chemotherapeutic targets are required. Recent investigations have uncovered the existence of a type II fatty acid biosynthesis (FAS-II) system in *Plasmodium falciparum* [1]. It is found in plants and most prokaryotes and consists of discrete enzymes that perform the individual reactions. Higher eukaryotes and yeast carry a type I system (FAS-I), which is structurally different with the biosynthetic enzymes integrated into a large multifunctional polypeptide. Fatty acids play a pivotal role in cells as metabolic precursors for biological membranes and energy stores, and inhibition of fatty acid biosynthesis has been validated as an excellent target in anti-microbial drug discovery. Several specific inhibitors of the FAS-II pathway are known, including isoniazid, triclosan and thiolactomycin. The latter two also inhibit the growth of *P. falciparum* [1], [2], [3], [4]. Recently, triclosan was identified as a potent inhibitor of the NADH-dependent *P. falciparum* enoyl-ACP reductase (also termed FabI), which is the key regulator of FAS-II, committing the final reduction step in chain elongation [2], [3]. This rendered the FabI enzyme an ideal target for the development of new anti-malarial drugs.

In order to discover anti-malarial agents from endemic Turkish plants, we studied *Phlomis brunneogaleata*, one of the 34 *Phlomis* species found in the flora of Turkey. The water-soluble portion of the total MeOH extract of the aerial parts of this plant was chosen for chemical investigations due to its anti-plasmo-

dial activity against a drug-resistant strain (K1) of *P. falciparum*. In this article, we describe the anti-plasmodial activity-guided purification and isolation of 16 metabolites, two of which (**1**, **2**) are new to the literature. The anti-protozoal activity of the single components against a broad panel of parasitic protozoa as well as their inhibitory potential towards purified enoyl-ACP reductase (FabI) of *P. falciparum* are also presented.

## Materials and Methods

### General experimental procedures

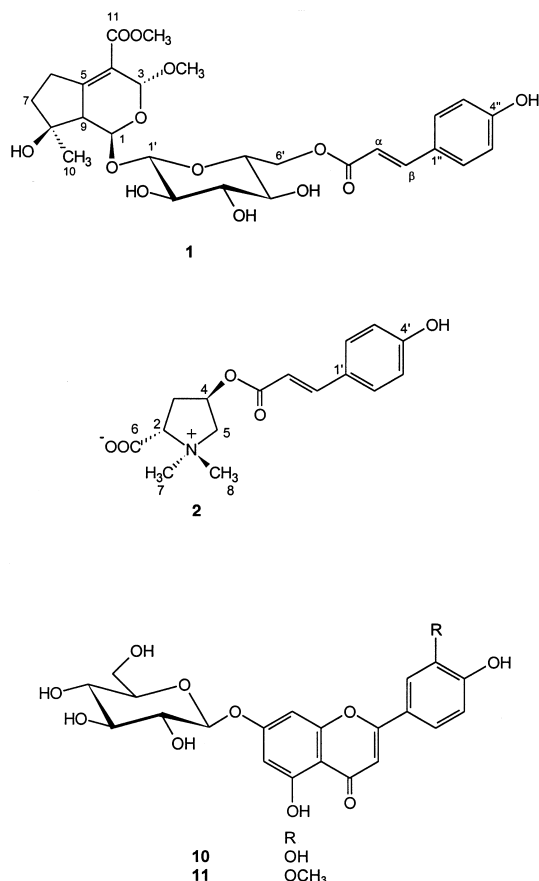
The NMR spectra were obtained on a Bruker Avance DRX 600 FT spectrometer operating at 600 (<sup>1</sup>H-NMR) and 150 (<sup>13</sup>C-NMR) MHz. The chemical shift values are reported as parts per million (ppm) units relative to tetramethylsilane (TMS). Mass spectra were taken on a Bruker Esquire-LC-MS (ESI mode) spectrometer. Optical rotations were recorded using an Autopol IV polarimeter. CC was carried out over silica gel (70–230 mesh, Merck) and polyamide (Fluka). MPLC separations were performed on a Labomatic glass column (2.6×46 cm; 3×24 cm, i.d.), packed with LiChroprep C<sub>18</sub>, using a Büchi 681 chromatography pump.

### Plant material

*Phlomis brunneogaleata* Hub.-Mor. (Lamiaceae) was collected from Gaziantep, Nurdagi, Turkey, in June 2002 and identified by one of us (A.A.D.). Voucher specimens have been deposited at the Herbarium of the Biology Department, Faculty of Science, Hacettepe University, Ankara, Turkey (AAD 10936).

### Extraction and isolation

The powdered aerial parts of *Phlomis brunneogaleata* (450 g) were extracted with MeOH (2×4 L, 5h) and then filtered. The filtrates were combined and evaporated to dryness under vacuum to afford 45 g crude extract (yield: 10%). The MeOH extract was suspended in H<sub>2</sub>O (50 mL), and then partitioned with CH<sub>2</sub>Cl<sub>2</sub> (4×100 mL). The H<sub>2</sub>O portion yielded 36 g extract upon concentration. An aliquot (35.5 g) of extract was placed on a column packed with polyamide (100 g). Elution with H<sub>2</sub>O (400 mL) and a stepwise gradient of MeOH in H<sub>2</sub>O (15–100% in steps of 15%, each 250 mL), yielded eight major fractions (frs. A–H). Fr. B (10.8 g) was subjected to RP-MPLC (LiChroprep C<sub>18</sub>; column dimensions: 2.6×46 cm), eluted with MeOH–H<sub>2</sub>O mixtures (0–60%, with increasing 5%, each 200 mL) to yield eight fractions, B<sub>1</sub>–B<sub>8</sub>. Fraction B<sub>2</sub> (100 mg) was rechromatographed on a silica gel (12 g) column (CHCl<sub>3</sub>–MeOH–H<sub>2</sub>O, 70:30:3 and 61:32:7, both 200 mL) to give **14** (31 mg). Fraction B<sub>3</sub> (50 mg) was applied to a silica gel (8 g) column [CHCl<sub>3</sub>–MeOH–H<sub>2</sub>O, 90:10:1 (100 mL), 800:20:2 (100 mL) and 70:30:3 (50 mL)] to obtain **13** (3 mg). Purification of fr. B<sub>5</sub> (159 mg) by silica gel (18 g) CC using CHCl<sub>3</sub>–MeOH–H<sub>2</sub>O (70:30:3, 400 mL) furnished **3** (7 mg) and **2** (7 mg). Fr. B<sub>6</sub> (250 mg) was chromatographed on a silica gel (20 g) column employing CH<sub>2</sub>Cl<sub>2</sub>–MeOH–H<sub>2</sub>O mixtures [80:20:2 (100 mL) and 70:30:3 (200 mL)] to afford fr. B<sub>6a</sub> (25 mg) and **7** (24 mg). Liriodendrin (**12**, 2 mg) was crystallized from fr. B<sub>6a</sub> in MeOH. Repeated chromatography of fr. B<sub>8</sub> (260 mg) on a silica gel (26 g) column utilising CH<sub>2</sub>Cl<sub>2</sub>–MeOH–H<sub>2</sub>O [90:10:1 (200 mL), 70:30:3 (200 mL) and 61:32:7 (100 mL)] yielded **8** (29 mg) and **6** (23 mg) respectively. Fr. D (1.6 g) was chromatographed by C<sub>18</sub>-MPLC (column dimensions: 3×24 cm) employing



an MeOH-H<sub>2</sub>O (15–65% with increasing 5%, each 200 mL) gradient to yield six major fractions, fr. D<sub>1</sub>–D<sub>6</sub>. Fr. D<sub>2</sub> (244 mg) was subjected to a silica gel (20 g) column using CH<sub>2</sub>Cl<sub>2</sub>-MeOH-H<sub>2</sub>O mixtures (90:10:1, 80:20:2 and 70:30:3, each 100 mL) to afford **15** (15 mg). Repeated chromatography of fr. D<sub>3</sub> (370 mg) on a silica gel (35 g) column [CH<sub>2</sub>Cl<sub>2</sub>-MeOH-H<sub>2</sub>O, 80:20:2 (100 mL) and 70:30:3 (200 mL)] yielded **4** (20 mg). Integrifolioside B (**9**, 3 mg) and brunneogaleatoside (**1**, 15 mg) were purified from fractions D<sub>5</sub> (50 mg) and D<sub>6</sub> (83 mg), respectively, in the same fashion [silica gel CC; CH<sub>2</sub>Cl<sub>2</sub>-MeOH-H<sub>2</sub>O (90:10:1, 80:20:2 and 70:30:3, each 100 mL for **9** and 90:10:1 (100 mL) and 80:20:2 (50 mL) for **1**]. Fraction F (950 mg) was likewise subjected to C<sub>18</sub>-MPLC (column dimensions: 3 × 24 cm) using stepwise gradients of MeOH (20–70% with increasing 5%; each 200 mL) in H<sub>2</sub>O to yield **16** (31 mg) and four main fractions, fr. F<sub>2</sub>–F<sub>5</sub>. Fr. F<sub>2</sub> (48 mg) was further applied to a silica gel (8 g) column [CH<sub>2</sub>Cl<sub>2</sub>-MeOH-H<sub>2</sub>O, 80:20:2 (100 mL) and 70:30:3 (50 mL)] to afford **5** (16 mg). Fr. F<sub>4</sub> (60 mg) was rechromatographed on a silica gel (6 g) column employing a CH<sub>2</sub>Cl<sub>2</sub>-MeOH-H<sub>2</sub>O mixture (80:20:2, 100 mL) to yield pure **10** (5 mg). Compound **11** (17 mg) was purified from fr. F<sub>5</sub> (85 mg) by using silica gel (12 g) CC and CHCl<sub>3</sub>-MeOH-H<sub>2</sub>O (85:15:1 and 80:20:2, both 100 mL) as eluents. Detection of the isolates by TLC [SiO<sub>2</sub>, solvent systems a: CHCl<sub>3</sub>-MeOH-H<sub>2</sub>O (70:30:3), b: CHCl<sub>3</sub>-MeOH-H<sub>2</sub>O (61:32:7), c:

CHCl<sub>3</sub>-MeOH-H<sub>2</sub>O (80:20:2), spray reagent: vanillin-H<sub>2</sub>SO<sub>4</sub>] Rf **1**:0.65 (c), **2**:0.26 (a), **3**:0.65 (a), **4**:0.42 (a), **5**:0.44 (a), **6**:0.33 (b), **7**:0.27 (b), **8**:0.35 (a), **9**:0.57 (a), **10**:0.36 (a), **11**:0.49 (a), **12**:0.43 (a), **13**:0.34 (a), **14**:0.24 (b), **15**:0.70 (a), **16**:0.52 (a).

### Physical and spectroscopic data

**Brunneogaleatoside (1)**: Amorphous powder;  $[\alpha]_D^{20}$ : –75.9° (c 0.1, MeOH). IR (KBr):  $\nu_{\max}$  = 3416, 1706, 1632, 1605, 1516 cm<sup>–1</sup>; UV (MeOH):  $\lambda_{\max}$  = 226, 304 nm; ESI-MS:  $m/z$  = 589 [M + Na]<sup>+</sup> (C<sub>27</sub>H<sub>34</sub>O<sub>13</sub>); <sup>1</sup>H-NMR (CD<sub>3</sub>OD, 600 MHz) and <sup>13</sup>C-NMR (CD<sub>3</sub>OD, 150 MHz): see Table 1.

(2*S*,4*R*)-2-carboxy-4-(*E*)-*p*-coumaroyloxy-1,1-dimethylpyrrolidinium inner salt (**2**): Colourless plates [from MeOH:MeCN (1:2)]; m.p. 239–241 °C;  $[\alpha]_D^{20}$ : +3.9° (c 0.1, MeOH). IR (KBr):  $\nu_{\max}$  = 3377, 1710, 1633, 1606, 1516 cm<sup>–1</sup>; UV (MeOH):  $\lambda_{\max}$  = 229, 304 nm; ESI-MS:  $m/z$  = 304 [M – H]<sup>–</sup>, 328 [M + Na]<sup>+</sup>, 633 [2M + Na]<sup>+</sup> (C<sub>16</sub>H<sub>19</sub>NO<sub>5</sub>); <sup>1</sup>H-NMR (DMSO-*d*<sub>6</sub>, 600 MHz) and <sup>13</sup>C-NMR (DMSO-*d*<sub>6</sub>, 150 MHz): see Table 2.

Specific rotation ( $[\alpha]_D^{20}$ ) values of the known compounds: **3**: –104° (c 0.215, MeOH); **4**: –84° (c 0.08, MeOH); **5**: –57° (c 0.09, MeOH); **6**: –78° (c 0.12, MeOH); **7**: –50° (c 0.13, MeOH); **8**: –63° (c 0.1, MeOH); **9**: –80° (c 0.05, MeOH); **10**: –48° (c 0.15, EtOH); **11**: –52°

Table 1 <sup>13</sup>C- and <sup>1</sup>H-NMR spectroscopic data and HMBC correlations for **1** (CD<sub>3</sub>OD, <sup>13</sup>C: 150 MHz; <sup>1</sup>H: 600 MHz)<sup>a</sup>

C/H		$\delta_c$ ppm	$\delta_H$ ppm, J (Hz)	HMBC (H→C)
1	CH	92.5	5.35 d (8.7)	C-3, C-5, C-9, C-1'
3	CH	98.8	5.30 s	C-1, C-4, C-5, 3-OCH <sub>3</sub>
4	C	123.4		
5	C	160.4		
6	CH <sub>2</sub>	29.9	2.72 m	C-4, C-5
7	CH <sub>2</sub>	40.2	1.83 m	C-5, C-6, C-8, C-9, C-10
			1.76 m	
8	C	79.3		
9	CH	56.2	2.70 d (8.7)	C-1, C-4, C-5, C-8
10	CH <sub>3</sub>	21.9	1.22 s	C-7, C-8, C-9
11	C	166.7		
3-OCH <sub>3</sub>	CH <sub>3</sub>	56.6	3.51 s	C-3
COOCH <sub>3</sub>	CH <sub>3</sub>	52.0	3.73 s	C-11
1'	CH	100.0	4.77 d (7.5)	C-1, C-5'
2'	CH	74.5	3.39 dd (8.6, 7.5)	C-3'
3'	CH	78.1	3.45 t (8.6)	C-2', C-4'
4'	CH	72.5	3.37 t (8.6)	C-3', C-5', C-6'
5'	CH	76.0	3.60 m	
6'	CH <sub>2</sub>	65.1	4.53 dd (11.8, 2.3)	C = O
			4.31 dd (11.8, 7.7)	C = O, C-5'
1''	C	127.3		
2''	CH	131.4	7.41 d (8.6)	C-3'', C-4'', C-5'', C-6'', C-β
3''	CH	117.0	6.76 d (8.6)	C-1'', C-4'', C-5'', C-β
4''	C	161.4		
5''	CH	117.0	6.76 d (8.6)	C-1'', C-2'', C-4'', C-6'', C-β
6''	CH	131.4	7.41 d (8.6)	C-1'', C-2'', C-4'', C-5'', C-β
α	CH	115.1	6.28 d (16.0)	C-1'', C-β, C = O
β	CH	147.0	7.59 d (16.0)	C = O, C-1'', C-2'', C-6'', C-α
C = O	C	169.1		

<sup>a</sup> All assignments are based on 2D NMR (DQF-COSY, HSQC, HMBC and ROESY).

Table 2  $^{13}\text{C}$  and  $^1\text{H}$  NMR spectroscopic data and HMBC correlations for **2** (DMSO- $d_6$ ,  $^{13}\text{C}$ : 150 MHz;  $^1\text{H}$ : 600 MHz)

C/H		$\delta_{\text{C}}$ ppm	$\delta_{\text{H}}$ ppm, J (Hz)	HMBC (H $\rightarrow$ C)
2	CH	75.0	4.13 dd (7.7, 11.0)	C-3, C-4, C-6, C-7, C-8
3 $\alpha$			2.72 ddd (15.0, 11.0, 8.1)	C-2, C-4, C-6
3 $\beta$	CH <sub>2</sub>	33.4	2.36 br. dd (15.0, 7.7, 2.0)	
4	CH	69.1	5.31 dddd (8.1, 7.7, 5.1, 2.0)	C = O, C-2
5 $\alpha$			4.22 dd (12.8, 7.0)	C-2, C-3, C-4, C-7, C-8
5 $\beta$	CH <sub>2</sub>	70.4	3.58 dd (12.8, 5.1)	
6	COO <sup>-</sup>	165.6		
7	(N-Me $\alpha$ )	47.0	3.12 s	C-2, C-5, C-8
8	(N-Me $\beta$ )	52.5	3.33 s	C-2, C-5, C-7
1'	C	124.7		
2'	CH	130.5	7.56 d (8.6)	C-3', C-4', C-5', C-6', C- $\beta$
3'	CH	116.0	6.83 d (8.6)	C-1', C-4', C-5', C- $\beta$
4'	C	160.5		
5'	CH	116.0	6.83 d (8.6)	C-1', C-3', C-4'
6'	CH	130.5	7.56 d (8.6)	C-3', C-4', C-5', C- $\beta$
$\alpha$	CH	113.1	6.39 d (16.0)	C = O, C-4, C-1', C- $\beta$
$\beta$	CH	145.9	7.63 d (16.0)	C = O, C-1', C-2', C-6', C- $\alpha$
C = O	C	166.2		

(*c* 0.09, EtOH); **12**:  $-17^\circ$  (*c* 0.06, MeOH); **13**:  $-79^\circ$  (*c* 0.14, MeOH); **14**:  $-120^\circ$  (*c* 0.045, MeOH); **15**:  $-29^\circ$  (*c* 0.09, MeOH); **16**:  $-97^\circ$  (*c* 0.09, MeOH).

Crystal data for compound **2** (see Fig. 1):  $\text{C}_{16}\text{H}_{19}\text{NO}_5 \cdot 2\text{H}_2\text{O}$ ,  $M_r = 341.36$ , monoclinic, space group  $P2_1$ ,  $a = 6.5137(1)$ ,  $b = 6.9192(2)$ ,  $c = 19.1825(5)$  Å,  $\beta = 91.293(1)^\circ$ ,  $V = 864.33(4)$  Å<sup>3</sup>,  $Z = 2$ ,  $D_x = 1.312$  g cm<sup>-3</sup>, crystal dimensions:  $0.05 \times 0.22 \times 0.28$  mm,  $T = 160$  K, Nonius KappaCCD area-detector diffractometer, Mo-K $\alpha$  radiation,  $\lambda = 0.71073$  Å,  $\mu = 0.103$  mm<sup>-1</sup>,  $\Theta_{\text{max}} = 30^\circ$ , 22 510 measured reflections, 2725 symmetry-independent reflections, 1899 reflections with  $I > 2\sigma(I)$ , no absorption correction. The struc-

ture was solved by direct methods with SIR92 and refined using SHELXL97 [5]. All non-H atoms were refined anisotropically. The hydroxy and water H-atoms were refined while restraining the water O-H and H $\cdots$ H distances. All remaining H atoms were placed in geometrically calculated positions and refined using a riding model. The refinement on  $F^2$  of 240 parameters using 2722 reflections and 8 restraints gave  $R(F)$  [ $I > 2\sigma(I)$  reflections] = 0.047,  $wR(F^2) = 0.124$ , (all reflections,  $S = 0.981$ ,  $\Delta\rho_{\text{max}} = 0.25$  e Å<sup>-3</sup>). A correction for secondary extinction was applied. The absolute configuration could not be determined crystallographically. Instead, the enantiomer used in the refinement was chosen to match that of a related compound [6], [7]. CCDC-225 408 contains the supplementary crystallographic data for this paper. These data can be obtained free of charge via [www.ccdc.cam.ac.uk/conts/retrieving.html](http://www.ccdc.cam.ac.uk/conts/retrieving.html) (or from the Cambridge Crystallographic Data Centre, 12 Union Road, Cambridge CB2 1EZ, UK; fax: +44-1223-336 033; e-mail: [deposit@ccdc.cam.ac.uk](mailto:deposit@ccdc.cam.ac.uk)).

### In vitro anti-protozoal and cytotoxic activity

Anti-parasitic assays for *Plasmodium falciparum*, *Trypanosoma cruzi* and *Trypanosoma brucei rhodesiense* as well as the cytotoxicity against rat skeletal myoblasts (L6 cells) were performed as previously described [8]. The assay for *Leishmania donovani* was done using the Alamar Blue assay as described for *T. b. rhodesiense*. Briefly, axenic amastigotes were grown in SM medium at pH 5.4 supplemented with 10% fetal bovine serum. 100  $\mu\text{L}$  of the culture medium with  $10^5$  amastigotes from axenic culture with or without a serial drug dilution were seeded in 96-well microtiter plates. Each drug was tested in duplicate and each assay was repeated once. After 72 hours of incubation 10  $\mu\text{L}$  of Alamar Blue (12.5 mg resazurin dissolved in 100 mL distilled water) were added to each well and the plates incubated for another 2 hours. Then the plates were read with a microplate fluorometer as previously described [8]. Artemisinin, benznidazole, melarso- pro, miltefosin and podophyllotoxin were used as positive controls. The IC<sub>50</sub> values of reference chemicals are shown in Table 3.

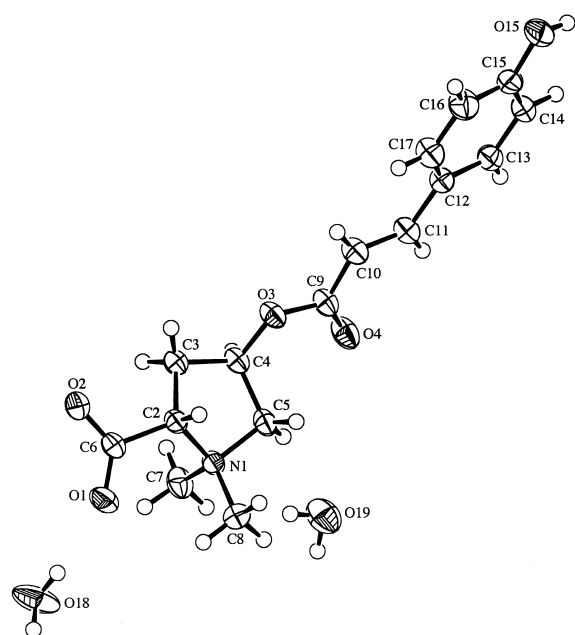


Fig. 1 3D-ORTEP projection of **2**·2H<sub>2</sub>O (crystallographic numbering, 50% probability ellipsoids).

### P. falciparum enoyl-ACP reductase inhibition assay

The protein was purified as described [2]. All measurements were performed on a Uvikon 941 Plus spectrophotometer (Kontron Instruments) in 1 mL of 20 mM Tris/HCl pH 7.4 and 150 mM NaCl. The compounds were dissolved in MeOH and tested at 10 µg/mL in the presence of 1 µg (20 nM) enzyme and 200 µM NADH. The reaction was started by addition of 50 µM crotonoyl-CoA. The reaction mixture was read spectrophotometrically for 1 min by following the oxidation of NADH to NAD<sup>+</sup> at 340 nm ( $\epsilon = 6.3 \text{ mM}^{-1} \text{ cm}^{-1}$ ). IC<sub>50</sub> values were estimated from graphically plotted dose-response curves. Triclosan was used as a positive control (IC<sub>50</sub> 50 nM = 14 ng/mL).

### Results

In a standard [<sup>3</sup>H]hypoxanthine uptake assay, the MeOH extract of the aerial parts of *Phlomis brunneogaleata* showed *in vitro* growth inhibitory activity against a chloroquine- and pyrimethamine-resistant strain (K1) of *P. falciparum* (IC<sub>50</sub>: 13.9 µg/mL). This extract was partitioned between H<sub>2</sub>O and CH<sub>2</sub>Cl<sub>2</sub>. The anti-malarial activity was tracked to the H<sub>2</sub>O-phase (IC<sub>50</sub>: 19.6 µg/mL), which was fractionated by polyamide CC. Three main polyamide fractions (B, D and F) retained the activity of the H<sub>2</sub>O extract. An anti-plasmodial activity-guided isolation protocol carried out on these fractions by employing RP-18 MPLC and silica CC afforded 16 metabolites. Herein we report the isolation, structure elucidation and biological activity profile of compounds **1** – **16**.

Brunneogaleatoside (**1**) was obtained as an optically active amorphous powder ([ $\alpha$ ]<sub>D</sub>: –75.9°, MeOH). Its molecular formula was established as C<sub>27</sub>H<sub>34</sub>O<sub>13</sub> on the basis of the positive-ion ESI-MS ( $m/z = 589$  [M + Na]<sup>+</sup>) and <sup>13</sup>C-NMR data (Table 1). The <sup>1</sup>H-NMR spectrum (Table 1) displayed signals due to a tertiary methyl ( $\delta$

1.22), two methylene ( $\delta$  2.72; 1.83 and 1.76), two acetal protons ( $\delta$  5.35 and 5.30), a methoxycarbonyl ( $\delta$  3.73) and an aliphatic methoxy ( $\delta$  3.51) functionalities. Moreover, the aromatic signals appeared as an AA'BB' system at  $\delta$  7.41 (2H) and 6.76 (2H) together with two olefinic protons observed as an AX system at  $\delta$  6.28 and 7.59 ( $J_{AX} = 16.0$  Hz) were indicative of an (*E*)-*p*-coumaroyl moiety. The anomeric proton signal at  $\delta$  4.77 along with the other sugar resonances at  $\delta$  3.37–4.53 suggested the presence of a  $\beta$ -glucopyranosyl unit in **1**. The <sup>13</sup>C-NMR spectrum of **1** contained 27 signals, six of which were attributed to a  $\beta$ -glucopyranosyl unit and nine of which were ascribed to an (*E*)-*p*-coumaric acid. A DEPT-135 experiment sorted the remaining 12 resonances arising from the aglycone moiety into four quaternary, three methine, two methylene, one methyl and two methoxy carbon atoms. All the <sup>1</sup>H- and <sup>13</sup>C-NMR chemical shifts of **1** (Table 1) were assigned by means of DQF-COSY, HSQC and HMBC experiments and clearly revealed that **1** has the basic aglycone skeleton of 3-epiphlomurin, an iridoid glycoside recently reported from *Phlomis aurea* [9]. 3-Epiphlomurin is a  $\Delta^{4,5}$  olefin (instead of  $\Delta^{3,4}$ ) and possesses an  $\alpha$ -methoxy function at C-3. The only significant difference between **1** and 3-epiphlomurin stems from the position of the  $\beta$ -hydroxy group in the cyclopentane ring. According to the chemical shift values of C-8 and Me-10, it is located at C-8 in **1**, whereas 3-epiphlomurin bears a hydroxy function at C-7. This interpretation was corroborated by the DQF-COSY spectrum where H<sub>2</sub>–6 ( $\delta$  2.72) and H<sub>2</sub>–7 ( $\delta$  1.83 and 1.76) appeared as the partners of one spin system. The other spin-coupled system was due to H-1 and H-9 of the iridoid aglycone. This left only the acyl function to be positioned. The downfield shifts for the H<sub>2</sub>–6' signals of the glucose unit and the long-range correlations (Table 1) between these signals and the carbonyl carbon atom of the *p*-coumaric acid revealed the site of esterification to be at C-6' (OH). The relative stereochemistry of the chiral centres in **1** was deduced by means of a ROESY experiment. ROE cross-peaks between H-3 and H-9 indicated that these pro-

Table 3 Biological activities of the metabolites of *Phlomis brunneogaleata* (IC<sub>50</sub> in µg/mL)

Compound	<i>Trypanosoma b. rhodesiense</i>	<i>Trypanosoma cruzi</i>	<i>Leishmania donovani</i>	<i>Plasmodium falciparum</i>	L6 cells
Reference	0.00098 <sup>a</sup>	1.06 <sup>b</sup>	0.102 <sup>c</sup>	0.0022 <sup>d</sup>	0.008 <sup>e</sup>
<b>1</b>	18.1	> 90	4.7	38.9	> 90
<b>2</b>	64.4	> 90	9.1	> 50	> 90
<b>3</b>	nt	nt	nt	nt	nt
<b>4</b>	14.2	> 90	8.7	> 50	37.1
<b>5</b>	6.2	> 90	9.2	37.5	55.4
<b>6</b>	5.8	> 90	11.4	> 50	70.1
<b>7</b>	8.9	> 90	13.1	> 50	> 90
<b>8</b>	28.1	> 90	9.5	> 50	> 90
<b>9</b>	> 100	> 90	8.4	> 50	> 90
<b>10</b>	60.6	> 90	1.1	2.4	> 90
<b>11</b>	88.7	> 90	4.1	5.9	> 90
<b>12</b>	34.4	> 90	11.6	> 50	> 90
<b>13</b>	> 100	> 90	11.2	> 50	> 90
<b>14</b>	18.9	> 90	7.0	> 50	> 90
<b>15</b>	16.8	> 90	8.8	42.8	84.1
<b>16</b>	21.4	> 90	7.3	> 50	> 90

<sup>a</sup> melarsoprol, <sup>b</sup> benznidazole, <sup>c</sup> miltefosin, <sup>d</sup> artemisinin, <sup>e</sup> podophyllotoxin, nt: not tested.



tons lie on the same side ( $\beta$ ) of the molecule. Significant correlations between H-1/Me-10 and H-1/OMe-3 showed them to be positioned on the other side ( $\alpha$ ) of the molecule. The  $\alpha$  orientation of the methoxy group at C-3 was further confirmed by comparing the chemical shift of C-1 ( $\delta_C$  92.5) with the epimeric compounds, phlomurin ( $\delta_C$  96.1) and 3-epiphlomurin ( $\delta_C$  92.3) [9].

Compound **2** was obtained as colourless plates (m.p. 239–241 °C,  $[\alpha]_D^{20}$ : +3.9°, MeOH). Its molecular formula was assigned as  $C_{16}H_{19}NO_5$  by negative and positive-ion ESI-MS ( $[M - H]^-$   $m/z$  = 304;  $[M + Na]^+$   $m/z$  = 328;  $[2M + Na]^+$   $m/z$  = 633) and  $^{13}C$ -NMR data (Table 2). From the  $^1H$ -NMR spectrum (Table 2), it was obvious that compound **2** also contained an (*E*)-*p*-coumaroyl moiety, in addition to two methylene ( $\delta$  4.22, 3.58;  $\delta$  2.72, 2.36), two methine ( $\delta$  5.31 and 4.13) and two *N*-methyl ( $\delta$  3.33 and 3.12) protons. The signal at  $\delta$  4.13 was indicative of a proton (H-2)  $\alpha$  to a quaternary nitrogen atom and a  $COO^-$  group, typical for a zwitterionic *N,N*-dimethylpyrrolidine ring [10]. This assumption was confirmed by long range correlations (Table 2) observed from H-2 to C-3, C-4, C-6 and both *N*-methyl signals. The chemical shift values of H-4 ( $\delta$  5.31) and C-4 ( $\delta$  69.1) implied the presence of an oxygen function at C-4. Furthermore, the cross peak between H-4 and the carbonyl carbon ( $\delta$  166.2) of the *p*-coumaroyl moiety suggested HO-C-4 to be the site of acylation. The complete assignment of the  $^1H$ -NMR signals and the determination of the relative stereochemistry at C-2 and C-4 were based on the analysis of the ROESY spectrum. Thus, the cross-peaks of H-2 ( $\delta_H$  4.13) with the signals at  $\delta_H$  2.36 (H-3 $\beta$ ), 3.58 (H-5 $\beta$ ) and 3.33 (N-Me-8) indicated their *cis*-relationship. Additional ROE correlations were observed between the proton pairs at  $\delta$  5.31 (H-4)/ $\delta$  4.22 (H-5 $\alpha$ ),  $\delta$  5.31 (H-4)/ $\delta$  3.12 (N-Me-7) and  $\delta$  2.72 (H-3 $\alpha$ )/ $\delta$  3.12 (N-Me-7). This finding and, in particular, the absence of dipolar coupling between H-2 and H-4 evidenced a *trans*-arrangement between H-2 and H-4 and therefore of the substituents at C-2 ( $COO^-$ ) and C-4 [(*E*)-*p*-coumaroyloxy]. Further analysis of the COSY, HSQC and HMBC spectra substantiated all proton and carbon signals (Table 2). Hence, **2** was established as the 4-(*E*)-*p*-coumaroyl ester of *trans*-4-hydroxyprolinebetaine (betonidine). A comparison of our NMR data with those published in the literature [7] indicated that the assignments of H-3 $\alpha$  and H-3 $\beta$  in [7] have to be interchanged. As compound **2** readily produced crystals of high quality, a low temperature X-ray crystal structure analysis was performed. The X-ray study confirmed the proposed relative stereochemical assignments for **2** (Fig. 1), but could not confirm the absolute configuration. The absolute configurations of (–)-betonidine (2*S*,4*R*), (+)-*ent*-betonidine (2*R*,4*S*), as well as that of the *cis*-diastereomers (–)-turicine (2*S*,4*S*) and (+)-*ent*-turicine (2*R*,4*R*) have been determined unambiguously by synthesis from the corresponding proline precursors [6]. Hence, the absolute configuration of **2** can be assigned after saponification and comparison of the  $[\alpha]_D^{20}$  values. However, due to the low quantity available of **2** and its consumption for the biological assays, this chiroptical correlation could not be performed. Since (4*R*)-hydroxy-L-proline is considered to be the predominant precursor of such betaines in Nature, we tentatively assign the (2*S*,4*R*)-configuration to **2**. Consequently, the structure of **2** was established as (2*S*,4*R*)-2-carboxy-4-(*E*)-*p*-coumaroyloxy-1,1-dimethylpyrrolidinium inner salt [(2*S*,4*R*)-1,1-dimethyl-4-(*E*)-*p*-coumaroyloxyproline inner salt].

In addition to these compounds, a known iridoid glycoside, ipolamiide (**3**) [11], six known phenylethanoid glycosides, verbascoside (**4**) [12], isoverbascoside (**5**) [11], forsythoside B (**6**) [11], echinacoside (**7**) [12], glucopyranosyl-(1 $\rightarrow$ G<sub>1</sub>-6)-martynoside (**8**) [13] and integrifolioside B (**9**) [14], two flavone glycosides, luteolin 7-*O*- $\beta$ -D-glucopyranoside (**10**) [15] and chrysoeriol 7-*O*- $\beta$ -D-glucopyranoside (**11**) [15], a lignan glycoside, liriodendrin (**12**) [16], an acetophenone glycoside, 4-hydroxyacetophenone 4-*O*-(6'-*O*- $\beta$ -D-apiofuranosyl)- $\beta$ -D-glucopyranoside (**13**) [17] and three caffeic acid esters, chlorogenic acid (**14**) [18], 3-*O*-caffeoylquinic acid methyl ester (**15**) [19] and 5-*O*-caffeoylshikimic acid (**16**) [20] were also isolated and identified by comparison of their 1D-NMR and MS data with those published in the literature. Since the specific rotation values of some of the known compounds are missing in the literature, the  $[\alpha]_D^{20}$  data of **3–16** in common solvents (MeOH or EtOH) are also listed in the Materials and Methods section.

The biological activities as well as the cytotoxic effects of compounds **1–2** and **4–16** on rat skeletal myoblasts (L6 cells) are shown in Table 3. Ipolamiide (**3**), the minor component of *P. brunneogaleata* could not be tested due to the limited amount isolated. Luteolin 7-*O*- $\beta$ -D-glucopyranoside (**10**) and chrysoeriol 7-*O*- $\beta$ -D-glucopyranoside (**11**) retained the *in vitro* activity of the crude extract against the chloroquine- and pyrimethamine-resistant *P. falciparum* (strain K1) with  $IC_{50}$  values of 2.4 and 5.9  $\mu$ g/mL, respectively. This prominent activity encouraged us to investigate the inhibitory activity of the isolates towards purified enoyl-ACP reductase (FabI) of *P. falciparum*, by means of an *in vitro* spectrophotometric assay. Luteolin 7-*O*- $\beta$ -D-glucopyranoside (**10**) displayed remarkable enzyme inhibitory potential towards plasmodial FabI enzyme ( $IC_{50}$ : 10  $\mu$ g/mL). All tested compounds exhibited a pronounced effect against axenic *L. donovani* amastigotes with  $IC_{50}$  values ranging from 1.1  $\mu$ g/mL to 13.1  $\mu$ g/mL. Noteworthy is that both flavonoid glycosides, **10** ( $IC_{50}$ : 1.1  $\mu$ g/mL) and **11** ( $IC_{50}$ : 4.1  $\mu$ g/mL) were the most potent leishmanicidal agents. The anti-protozoal activity of the isolates was also evaluated against the trypomastigote forms of two *Trypanosoma* species. Although none were active against *T. cruzi*, all *P. brunneogaleata* metabolites, except for **9** and **13**, showed appreciable trypanocidal effect towards *T. brucei rhodesiense* (Table 3). Particularly active compounds were **5**, **6** and **7** with  $IC_{50}$  values of 6.2, 5.8 and 8.9  $\mu$ g/mL, respectively. As shown in Table 3, none of the isolates displayed significant toxicity on the respective mammalian host cells (L6).

## Discussion

It has long been believed that the malaria parasite, *Plasmodium* sp., is unable to make its own fatty acids, depending instead on scavenged fatty acids from the host erythrocyte and serum [21]. The discovery of a type II fatty acid biosynthesis (FAS-II) in *Plasmodium* was therefore surprising, as this pathway had been found only in plants and prokaryotes. The current molecular and biochemical data show that in *Plasmodium*, FAS-II is the only fatty acid pathway whose enzymatic components reside in the apicoplast, a unique plastid organelle derived from a cyanobacterial endosymbiont [1], [4], [21]. The individual condensation, reduction and dehydration reactions in type II fatty acid

biosynthesis are carried out by separate enzymes. The final reduction step in each elongation process is catalyzed by a single enzyme, enoyl-ACP reductase (FabI). This key regulatory effect of FabI in the fatty acid biosynthesis of *P. falciparum*, as well as the absence of the whole FAS-II pathway in humans, make this enzyme an excellent target for anti-malarial drug discovery. Triclosan, a widely used antibacterial agent, has emerged as the most powerful inhibitor of this enzyme [3] (in this study  $IC_{50}$ : 14 ng/mL). Triclosan potently inhibits the growth of *P. falciparum* *in vitro* ( $IC_{50}$ : 0.2  $\mu$ g/mL to 2  $\mu$ g/mL, depending on the parasite strain tested [4]), and also *in vivo*, in the *P. berghei* mouse model [3]. So far, only two natural products, cerulenin and thiolactomycin, both of fungal origin, are known to inhibit the plasmodial FAS-II. However, the major targets of these compounds are FabB/FabF and FabH [1], [21], and not FabI. Thus, luteolin 7-*O*- $\beta$ -D-glucopyranoside (**10**) isolated in this study appears to be the first plasmodial FAS-II inhibiting natural product, specifically and significantly targeting the malarial FabI enzyme ( $IC_{50}$ : 10  $\mu$ g/mL). Luteolin 7-*O*- $\beta$ -D-glucopyranoside (**10**) also inhibits the incorporation of [ $^3$ H]hypoxanthine into *Plasmodium* more efficiently ( $IC_{50}$ : 2.4  $\mu$ g/mL) than cerulenin ( $IC_{50}$ : 4.5  $\mu$ g/mL) or thiolactomycin ( $IC_{50}$ : 10.3  $\mu$ g/mL) [3], [21]. It is interesting that chrysoeriol 7-*O*- $\beta$ -D-glucopyranoside (**11**), a 3'-methoxy derivative of **10**, has no inhibitory activity towards FabI, indicating the importance of an *ortho*-diphenol structure for enzyme interaction. Compound **11** has a broad anti-parasitic spectrum and is also active against *L. donovani* ( $IC_{50}$ : 1.1  $\mu$ g/mL), the causative agent of visceral leishmaniasis.

Betaines are common within the family Lamiaceae and are found in large amounts in the members of the subfamily Lamioideae, to which the genus *Phlomis* also belongs. These compounds have been shown to have chemotaxonomic significance for Lamiaceae, especially at a generic level [22]. Caffeic acid esters are also very widely distributed in Lamiaceae and are of taxonomic importance. To our knowledge, this is the first report of a betaine-phenylpropanoic acid ester from a natural source. Such betaine esters might be useful chemotaxonomic markers in the future. This is also the first report on the isolation of the phenylethanoid glycosides **7** and **8**, the acetophenone glycoside **13** and the caffeic acid esters **15** and **16** from the genus *Phlomis*.

## Acknowledgements

Dr. Helmut Legerlotz Stiftung (D.T.) and the Scientific and Technical Research Council of Turkey (TUBITAK, Project No: SBAG-2304, H.K., I.Ç.) are gratefully acknowledged for financial support.

## References

- Waller RF, Keeling PJ, Donald RG, Striepen B, Handman E, Lang-Unnasch N et al. Nuclear-encoded proteins target to the plastid in *Toxoplasma gondii* and *Plasmodium falciparum*. *Proc Natl Acad Sci USA* 1998; 95: 12352–7
- Perozzo R, Fidock DA, Kuo M, Sidhu AS, Valiyaveetil JT, Bittman R et al. Structural elucidation of the specificity of the antibacterial agent triclosan for malarial enoyl acyl carrier protein reductase. *J Biol Chem* 2002; 277: 13106–114
- Surolia N, Surolia A. Triclosan offers protection against blood stages of malaria by inhibiting enoyl-ACP reductase of *Plasmodium falciparum*. *Nature Med* 2001; 7: 167–73
- McLeod R, Muench SP, Rafferty JB, Kyle DE, Mui EJ, Kirisits MJ et al. Triclosan inhibits the growth of *Plasmodium falciparum* and *Toxoplasma gondii* by inhibition of apicomplexan FabI. *Int J Parasitol* 2001; 31: 109–13
- Sheldrick GM. SHELXL97, Program for the refinement of crystal structures. University of Göttingen, Germany: 1997
- Patchett AA, Witkop B. Studies on hydroxyproline. *J Am Chem Soc* 1957; 79: 185–92
- Blunden G, Gordon SM, Crabb TA, Roch OG, Rowan MG, Wood B. NMR spectra of betaines from marine algae. *Magn Res Chem* 1986; 24: 965–71
- Sperandeo NR, Brun R. Synthesis and biological evaluation of pyrazolynaphthoquinones as new potential antiprotozoal and cytotoxic agents. *ChemBioChem* 2003; 4: 69–72
- Kamel MS, Mohamed KM, Hassanean HA, Ohtani K, Kasai R, Yamasaki K. Iridoid and megastigmane glycosides from *Phlomis aurea*. *Phytochemistry* 2000; 55: 353–7
- Chini C, Bilia AR, Keita A, Morelli I. Protoalkaloids from *Boscia angustifolia*. *Planta Medica* 1992; 58: 476
- Ersöz T, Harput ÜI, Çalis I, Dönmez AA. Iridoid, phenylethanoid and monoterpene glycosides from *Phlomis siehana*. *Turk J Chem* 2002; 26: 1–8
- Abougazar H, Bedir E, Khan IA, Çalis I. Wiedemanniosides A – E: New phenylethanoid glycosides from the roots of *Verbascum wiedemannianum*. *Planta Medica* 2003; 69: 814–9
- Otsuka H. Phenylethanoids from *Linaria japonica*. *Phytochemistry* 1993; 32: 979–81
- Saracoglu I, Varel M, Hada J, Hada N, Takeda T, Dönmez AA et al. Phenylethanoid glycosides from *Phlomis integrifolia* Hub.-Mor. *Z Naturforsch* 2003; 58c: 820–5
- Markham KR, Chari VM.  $^{13}$ C NMR Spectroscopy of Flavonoids. In: *The Flavonoids: Advances in Research* (Harborne JB; Mabry TJ eds.). London: Chapman and Hall, 1982: pp 19–132
- Chaudhuri RK, Sticher O. New iridoid glycosides and a lignan diglucoside from *Globularia alypum* L. *Helv Chim Acta* 1981; 64: 3–15
- Lu Y, Foo LY. Flavonoid and phenolic glycosides from *Salvia officinalis*. *Phytochemistry* 2000; 55: 263–7
- Cheminat A, Zawatzky R, Becker H, Brouillard R. Caffeoyl conjugates from *Echinacea* species: Structures and Biological activity. *Phytochemistry* 1988; 27: 2787–94
- Peng LY, Mei SX, Jiang B, Zhou H, Sun HD. Constituents from *Lonicera japonica*. *Fitoterapia* 2000; 71: 713–5
- Veit M, Weidner C, Strack D, Wray V, Witte L, Czygan FC. The distribution of caffeic acid conjugates in the Equisetaceae and some ferns. *Phytochemistry* 1992; 31: 3483–5
- Waller RF, Ralph SA, Reed MB, Su V, Douglas JD, Minnikin DE et al. A type II pathway for fatty acid biosynthesis present drug targets in *Plasmodium falciparum*. *Antimicrob Agents Chemother* 2003; 47: 297–301
- Blunden G, Yang M-H, Yuan Z-X, Smith BE, Patel A, Cegarra JA et al. Betaine distribution in the Labiatae. *Biochem Syst Ecol* 1996; 24: 71–81